Published in final edited form as:

Cancer Res. 2017 August 15; 77(16): 4317–4327. doi:10.1158/0008-5472.CAN-16-3011.

Loss of *FAM46C* promotes cell survival in myeloma

Yuan Xiao Zhu[1], **Chang-Xin Shi**[1], **Laura A. Bruins**[1], **Patrick Jedlowski**[1], **Xuewei Wang**[2], **K. Martin Kortüm**[1], **Moulun Luo**[3], **Jonathan M. Ahmann**[1], **Esteban Braggio**[1], and **A. Keith Stewart**[1,4]

[1]Division of Hematology, Mayo Clinic Scottsdale, Arizona, USA

[2]Division of Biomedical Statistics and Informatics, Department of Health Sciences Research, Mayo Clinic Rochester, Minnesota, USA

[3]Center for Metabolic and Vascular Biology, Arizona State University, Tempe, Arizona, USA

[4]Center for Individualized Medicine, Mayo Clinic, Rochester, Minnesota, USA

Abstract

FAM46C is one of the most recurrently mutated genes in multiple myeloma (MM), however its role in disease pathogenesis has not been determined. Here we demonstrate that wild type (WT) *FAM46C* overexpression induces substantial cytotoxicity in MM cells. In contrast, *FAM46C* mutations found in MM patients abrogate this cytotoxicity, indicating a survival advantage conferred by the *FAM46C* mutant phenotype. WT FAM46C overexpression downregulated *IRF4*, *CEBPB*, and *MYC* and upregulated immunoglobulin (Ig) light chain and *HSPA5*/*BIP*. Furthermore, pathway analysis suggests that enforced *FAM46C* expression activated the unfolded protein response (UPR) pathway and induced mitochondrial dysfunction. CRISPR-mediated depletion of endogenous *FAM46C* enhanced MM cell growth, decreased Ig light chain and BIP expression, activated ERK and anti-apoptotic signaling, and conferred relative resistance to dexamethasone and lenalidomide treatments. Genes altered in *FAM46C*-depleted cells were enriched for signaling pathways regulating estrogen, glucocorticoid, B cell receptor signaling, and ATM signaling. Together these results implicate FAM46C in myeloma cell growth and survival and identify *FAM46C* mutation as a contributor to myeloma pathogenesis and disease progression via perturbation in plasma cell differentiation and endoplasmic reticulum homeostasis.

Keywords

FAM46C; multiple myeloma; immunoglobulin; ER stress

Introduction

The molecular basis of multiple myeloma (MM) is still incompletely understood. Cytoband 1p12 is deleted in approximately 20% of MM patients and has been reported to associate

Correspondence: A. Keith Stewart, MD, Division of Hematology, Mayo Clinic Arizona, 13400 E. Shea Blvd., Scottsdale, AZ 85259, stewart.keith@mayo.edu, T: 480-301-4279, F: 480-301-8387.

Conflict-of-interest disclosure

The authors declare no competing financial interests

with shorter overall survival (OS) (1). The target gene on 1p12, as suggested by the presence of recurrent homozygous deletions, is *FAM46C*(2). Several studies have reported *FAM46C* mutations in 5% to 13% of primary MM tumors(3–7), implying its pathogenic relevance. We have previously suggested that *FAM46C* mutations are less frequent in newly diagnosed MM patients harboring deletion 17p(8), potentially inferring some overlap in function. Moreover, acquisition of mutations was observed in longitudinal analysis in MM patients(9), suggesting that *FAM46C* loss of function is a progression event in MM.

FAM46C belongs to the nucleotidyltransferase superfamily(10), together with 3 other FAM46 proteins (FAM46A, B and D). A recent study, using a combination of bioinformatics analyses, proposed that FAM46 proteins are novel eukaryotic non-canonical poly (A) polymerases and may be involved in the regulation of gene expression, cell differentiation and development of several malignancies(11). In a cell-based assay, *FAM46C* was identified to enhance replication of some viruses, including yellow fever virus, in response to type I interferon(12). *FAM46C* expression is also reported to correlate with the expression of ribosomal proteins and the eukaryotic initiation and elongation factors involved in protein translation in myeloma cells (3).

In the present study, we conducted a comprehensive analysis of *FAM46C* in MM. We found that enforced *FAM46C* expression in human MM cell lines (HMCLs) induced MM cytotoxicity and enhanced drug sensitivity, whereas introduction of *FAM46C* mutants has no such anti-MM activity. Furthermore, *FAM46C* CRISPR depletion enhanced MM cell growth, survival and decreased immunoglobulin (Ig) expression in MM cells.

Materials and Methods

Cells and Reagents

HMCLs were either obtained from ATCC (Manassas, VA) or provided by Dr. Leif Bergsagel's laboratory from 2014 to 2016. An initial genetic analysis of these lines (CNV analysis) established a baseline, identifying fingerprint (developed by Dr. Leif Bergsagel and Dr. Jonathan Keats). The identity of cell lines was confirmed using CNV analysis each time samples are removed from liquid nitrogen storage for propagation. All cell lines taken from liquid nitrogen were thawed and maintained in RPMI-1640 media, supplemented with 5% of sterile fetal calf serum and antibiotics. All cell lines were maintained for three to four weeks (8 –10 passages) before starting experiment and they were tested negative for mycoplasma at the beginning and during the experiments (using mycoplasma detection kit from Lonza, Rockland, ME). Anti-Flag was from Sigma-Aldrich (St. Louis, MO). Anti-IRF4, anti-CDK6, anti-PARP, anti-BIP, anti-Caspase 8, anti-CHOP, Anti-Lamin A/C, anti-p ERK1/2, anti ERK1/2 and anti-BCL2 were from Cell Signaling Technology (Danvers, MA). Anti-MYC antibody was from Epitomics (Burlingame, CA). Anti-FAM46C antibodies were from Abcam (Cambridge, MA) and Proteintech (Chicago, IL) and their specificities were validated by western blot of the lysates either from the cells without FAM46C expression or with exogenous FAM46C expression (shown in figures). Anti-Ig lambda (λ) and kappa (κ) chain antibodies were from Abcam (Cambridge, MA) and Santa Cruz Biotechnology (Dallas, TX) respectively. Anti-HA was from Covance (Hollywood, FL). Dexamethasone (Dex) was from Sigma-Aldrich (St. Louis, MO). Lenalidomide (Len) and bortezomib were

from LC Laboratories (Woburn, MA). All Taqman probes (BIP and MAGED1) used in real time PCR were from Thermo Fisher Scientific (Waltham, MA).

Preparation of lentiviral virus expressing FAM46C or other proteins and infection of myeloma cells

Human wild-type (WT) FAM46C cDNA was purchased from Thermo Scientific (Rockford, IL) and were sub-cloned into a lentiviral expression vector, pCDH-CMV-MCS-EF1-copGFP (System Bioscience, Mountain View, CA). FAM46C tagged with Flag or HA at its C-terminal was generated by PCR method and inserted into the modified pCDH-CMV-MCS-EF1-copGFP or pCDH-CMV-MCS-EF1-puro. All FAM46C mutants were amplified with specific primers (supplemental table 1) from wild type cDNA by PCR methods and were cut with appropriate restriction enzymes and then subcloned into pCDH-CMV-MCS-EF1-copGFP. Human *PSMC6* cDNA was from Thermo Scientific and PSMC6 tagged with HA at its C-terminal was generated by PCR and inserted into the modified pCDH-CMV-MCS-EF1-puro. All constructs were verified by sequencing. pCDH-EF1-CYMR-T2A-puro was from System Bioscience. Lentivirus harboring control vector and all expression constructs were generated and used to infect HMCLs. The infection efficiency was measured by flow cytometry analysis of GFP expression at day 3 after infection. Overexpression of FAM46C was confirmed by immunoblotting assay.

Knockout of *FAM46C* using CRISPR-Cas9 technology

Lentiviral constructs expressing CRISPR associated protein 9 (Cas9) and guide RNAs (gRNAs) were originally generated from Feng Zhang's lab(13, 14) and were obtained from Addgene (Cambridge, MA). The gRNA expressing plasmid was modified by subcloning gRNA expressing cassette into pCDH-CMV-MCS-EF1-copGFP or pCDH-CMV-MCS-EF1-Puro. We first established HMCLs stably expressing Cas9 by infection of HMCLs with lentivirus expressing Cas9, followed by selecting with blasticidin. A total of seven guide RNAs (gRNAs) were selected using the online CRISPR design tool on Fang Zhang's lab website, including: #1 AAGTTGCCTCGTCCGTGGAT; #2 GAACTCAAACTGACGCCGAA; #3 GTTGTACCTATCCACGGACG; #4 TCGTCCAGACCGTCCGCAGT; #5 TTGGAAAGTTGCCTCGTCCG; #6 ATCCCAGTTGAGCACGCTGA and #7 GCTGAAGGACATGCAATCCC. They were synthesized and cloned into the BbsI-digested plasmid containing the entire guide RNA scaffold. Lentivirus harboring non-targeting vector (NS) and all gRNA expression constructs were generated and used to infect HMCLs. The infection efficiency was measured by flow cytometry analysis of GFP expression at day 3 after infection. The expression of FAM46C was evaluated by immunoblotting assay. The single clones that have *FAM46C* knockout were selected using limited dilution and immunoblotting assay.

Array-Based Comparative Genomic Hybridization (aCGH)

DNA was extracted from mononuclear cells using Puregene kit (Qiagen) and the manufacturer's recommended protocol. All HMCLs were run using the Human 244K microarray (Agilent Technologies). The digestion, labeling and hybridization steps were performed as previously described with minor modifications(15). Copy number

abnormalities (CNA) were calculated using 2 probe and 0.2 log2 filters and aberration detection module (ADM)-1 algorithm(16) with a threshold of 9.0.

DNA sequencing

DNA was extracted using the Qiagen AllPrep DNA/RNA Mini Kit according to the manufacturer's recommendations. In order to screen HMCLs for mutations as well as to confirm the introduction of CRISPR-mediated *FAM46C* mutations, we employed the Ion Torrent semiconductor sequencing platform (PGM, Life Technologies, Carlsbad, CA, USA) (8), using 20 ng of starting DNA per sample. The coding regions of *FAM46C* were amplified in 200-bp libraries using 4 pairs of customized oligos from Ion AmpliSeq Designer, Life Technologies (#1 Fwd primer CGAGCTGCTTTGCCATGTAGAA and #1 Rev primer CATGGAAGATTAGGTCCAGGTCTTTG; #2 Fwd primer GCCACGTTTTGGTCAAAGACAAT and #2 Rev primer GAAGAAAAGCAAAGAATCCAGGATGATTT; #3 Fwd primer GGCGTCAGTTTGAGTTCAGTGT and #3 Rev primer TCAGCGAAGTGGTTTTGAAGGT; #4 Fwd primer GACATCCTTGAACAGCAGAGGAA and #4 Rev primer GTGGAAACCCTCAGGTCTCAAG). Libraries were templated and enriched using IonOneTouch2 and IonOneTouch ES automated systems, respectively. Samples were sequenced using the 318^{TM} chip (ThermoFisher). Overall, we obtained an average coverage depth of 500X. Raw data was aligned and indexed in BAM and BAI files using the IonTorrent suite. Variants were called using IonTorrent Somatic VariantCaller version 4.6.0.7 and low stringency settings (ThermoFisher). VCF files were annotated using a standalone application developed by the Mayo Clinic Bioinformatics Program called BioR (Biological Annotation Data Repository)(17). BioR includes gene annotation from NCBI/Ensembl and UCSC, Gene annotated pathways (KEGG), tissue specificity, GeneCards and Gene Ontology (GO), dbSNP, GWAS catalog, HapMap, and 1000 Genomes. Somatic variants with a Mapping Quality <20 or read depth <10X were removed. Finally, variants of significant interest were visually inspected using Integrative Genomics Viewer (18, 19).

Cell viability and apoptosis assay

HMCLs were cultured in RPMI 1640 media, supplemented with 5% of sterile fetal calf serum and antibiotics. Cell viability was measured by 3-(4,5-dimethylthiazol)-2,5-diphenyl tetrazolium (MTT) dye absorbance according to the manufacturer's instructions (Boehringer Mannheim). MTT assay was set up either in the absence or presence of drugs (such as Len and Dex). Each experimental condition was performed in triplicate and most of them were repeated at least twice.

Apoptosis was determined by flow cytometry analysis using the TACS Annexin V-FITC apoptosis detection kit (BD) according to the manufacturer's instructions. Briefly, myeloma cells were harvested at day 3 after infection with lentivirus expressing wild type *FAM46C* or vector alone, washed with PBS and stained with Annexin V–FITC and PI, followed by analysis on CyAn ADP flow cytometer (DaKo, Denmark)

mRNA sequencing (mRNA-seq)

MM1.S and KMS11 cells were harvested at day 3 after infection with lentivirus harboring either control vector or wild-type FAM46C-expressing cassette. Total RNA was prepared using RNeasy plus kit under the protocols of the manufacturer (Qiagen, Valencia, CA). mRNA-seq experiment was performed at the medical genome facility in Mayo Clinic, Rochester. Base calling with raw sequencing data was performed with Illumina's RTA (v. 1.17.21.3). Each individual sample in this study has at least 80 million total reads. An internally developed RNA-seq analysis workflow (MAPRSeq v2.0.0)(20) was used to perform read alignment, quality control and expression quantification. Specifically, pair-ended reads were aligned by TopHat (v2.0.12)(21) against hg19 genome build, quality control across genes was performed with RSeQC (v2.3.2)(22), gene counts were generated with featureCounts from Subread package (http://subread.sourceforge.net/, v1.4.4)(23). For each sample, gene counts were normalized against gene lengths to generate RPKM (reads per kilobase pair per million mapped reads) as expression levels. Differential analysis was then performed by Student's t-test for two comparisons (MM1.S FAM46C vs. control, KMS11 FAM46C vs. control) and the complete dataset is accessible through GEO series accession number GSE99358. Genes were determined as differentially expressed based on the criteria (RPKM >=3 in at least two samples, p-value <=0.05 and fold change >= 1.5) and submitted to Ingenuity Pathway Analysis (IPA, http://www.ingenuity.com/) for pathway enrichment analysis.

Immunoblotting analysis

Western Blot was performed according to manufacturer's protocol. Equal amounts of protein were subjected to sodium dodecyl sulfate polyacrylamide gel electrophoresis (SDS-PAGE) gels followed by transfer to PVDF membranes. Membranes were probed with primary antibodies overnight and then washed and incubated with horseradish peroxidase (HRP)-conjugated-secondary antibodies. Detection was performed by the Enhanced Chemical Luminescence (ECL) method. When probing for multiple targets or validating equal amount of protein load, stripping and re-probing a single membrane were conducted. In the case of protein re-probed was absent, the same samples were usually re-run to validate the result.

Fractionation of cytoplasmic protein and nuclear extract was performed extraction kit (Thermo Scientific, Rockford, IL). Equal amounts of protein were subjected to immunoblotting analysis as described above.

Real-time PCR (qPCR)

Total RNA and cDNA were prepared using RNeasy plus kit and QuantiTect Reverse Transcription kit under the protocols of the manufacturer (Qiagen, Valencia, CA). RT-PCR amplification was carried out with 80 ng of cDNA in 11.25 μL of reaction mixture (TaqMan Universal PCR Master Mix with predesigned probes). Data quantification was performed by the $2^{-\Delta\Delta Ct}$method (24).

Gene expression profiling

To assess the gene expression changes induced by FAM46C depletion, three samples, including OCIMY5 cells harboring, respectively, control, FAM46C gRNA #1 and FAM46C

#6 gRNA, were harvested and processed for gene expression analysis. The gene expression profiles were generated from total RNA labeled using the Affymetrix OneStep IVT labeling procedure and hybridized to the Affymetrix human HTA 2.0 genechip. Gene expression values were extracted from the raw CEL files using Affymetrix Expression Console software (with SST-RMA normalization approach and log-transformation). Differentially expressed genes between FAM46C knockout and NS were then identified using Affymetrix Transcriptome Analysis Console (with one-way ANNOVA approach), with p-value cutoff at 0.05 and fold change cutoff at 1.5. The complete dataset is accessible through GEO series accession number GSE99358. Ingenuity Pathway Analysis was used to perform pathway enrichment analysis from differentially expressed genes.

Results

FAM46C encodes a cytoplasmic protein and is frequently mutated in MM

We screened nine HMCLs using aCGH and DNA sequencing and showed that *FAM46C* is deleted and/or mutated in five of the nine lines studied. Cell line LP1 carries a *FAM46C* biallelic deletion. KMS11 and OCIMY5 have monoallelic deletions, and OPM2 and MM1.S carry both monoallelic deletion and missense mutations in the remaining allele (Figure 1A). FAM46C with a HA tag at its C-terminal was introduced into LP1 cells to validate specificity of an anti-FAM46C antibody. As expected, no endogenous FAM46C protein was detected in LP1 (Figure 1B). On the other hand, exogenous wild-type FAM46C was detected by both anti-HA and anti-FAM46C immunoblotting. In addition to the full-length protein, a short FAM46C protein was also identified by the anti-FAM46C antibody. With the exception of LP1, we detected both full-length and short FAM46C in all remaining HMCLs (Figure 1C). Furthermore, we demonstrated the cytoplasmic localization of FAM46C in four HMCLS (Figure 1D).

FAM46C overexpression results in myeloma cytotoxicity

To better understand the role of FAM46C, we introduced lentiviruses expressing either *FAM46C* WT or control vector into three HMCLs harboring known genomic abnormalities affecting *FAM46C*. Infection efficiency, measured at day 3, was greater than 80% in all cases (Figure 2A). At day 6 after infection, MTT assay indicated that both untagged and tagged-FAM46C induced a substantial reduction of cell viability. The reduction was particularly noticeable in MM1.S, which harbors a *FAM46C* hemizygous missense mutation (Figure 2B). Both untagged and tagged-FAM46C showed similar anti-MM activity although their expression levels are different (Figure 2C).

At day 3 after infection, FAM46C overexpression induced a relative increase in apoptosis of 8% and 16% in KMS11 and MM1.S, respectively (Figure 2D). Overall, *FAM46C* induced a significant cytotoxicity in seven of nine tested HMCLs (Figure 3A–B). The 2 HMCLs not showing cytotoxicity were FR4 and JJN3, both of which contain endogenous non-mutated *FAM46C*. In four non-myeloma cell lines, three were unaffected but one melanoma cell line, win-226 also showed a substantial reduction of viability.

In order to determine whether FAM46C-induced cytotoxicity is protein specific, we utilized three lentiviral controls (empty vector and irrelevant proteins including PSMB6 and CmyR repressor). Only *FAM46C* overexpression induced a substantial cell viability reduction in MM cells when compared with controls (Figure 3C–D). We further demonstrated that FAM46C-induced cytotoxicity is dose dependent (Figure 3E–F).

We also identified HMCLs that survived FAM46C-induced cytotoxicity and stably expressed FAM46C. These cells were however less fit as exhibited by an increased sensitivity to anti-myeloma therapy. Specifically, 2–3 weeks after infection, KMS11 and OPM2 cells with FAM46C WT overexpression showed greater sensitive to dexamethasone and lenalidomide than control virus infected cells (supplementary figure 1). On the other hand, RPMI8226, which is inherently resistant to lenalidomide, only showed a significantly improved response to dexamethasone.

Expression analysis identified a subset of genes altered in *FAM46C* overexpressing cells, including *IRF4*

To understand the underlying mechanism for FAM46C-mediated anti-myeloma activity, mRNA-seq profile was compared in MM1.S and KMS11 cells before and after introduction of *FAM46C*. At day 3 after infection, 422 genes were significantly altered (113 down and 309 upregulated) in both FAM46C overexpressing cell lines (supplementary table 2). Among the most downregulated genes, we identified genes associated with myeloma survival and growth, including *IRF4*(25), *CEBPB(26) and IL-6R*. In MM1.S, down-regulated genes also included *AURKA*, *AURKB*(27–29) and *IRF4* downstream targets, such as *CDK6* and *BCL2*(25). Among *FAM46C* up-regulated genes, we identified genes associated with the unfolded protein response (UPR) (including *HSPA5/BIP* and *PDIA4*), B cell biology (including Ig λ chain) and additional genes involved in other malignancies (e.g. *EMP3,* BPXIP1, *MAGED1* and *MAGED2*). Pathway analysis demonstrated mitochondrial dysfunction, UPR, antigen presentation pathway and NRF2-mediated oxidative stress response as the top canonical pathways affected (Table 1 and supplementary table 3). The finding of up-regulation of BIP, Immunoglobulin light chain production and multiple genes involved in the UPR after FAM46C introduction, suggest that FAM46C overexpression activates the endoplasmic reticulum (ER) stress pathway.

FAM46C overexpression induced IRF4 downregulation, Ig light chain upregulation and UPR activation

In order to further confirm the connection of gene expression changes with FAM46C-induced MM cytotoxicity, three HMCLs were analyzed for protein expression of FAM46C targets at days 2, 3 (immunoblotting), and 6 (cell viability assay) after lentivirus infection. Consistent with RNAseq data, IRF4 and MYC were significantly downregulated in the two cell lines exhibiting cytotoxicity. Ig light chain and BIP were upregulated after introduction of exogenous FAM46C (Figure 4A–B). Furthermore, IFR4 and MYC downregulation was correlated with cell viability reduction. IRF4 and MYC downregulation occurred before the apoptotic signal, as shown by Caspase 8 and PARP cleavage (Figure 4B). OPM2, which had very little change in IRF4 or MYC level, underwent less cytotoxicity (Figure 4A and B).

We further validated our data in three HMCLs infected by lentivirus harboring control vector and FAM46C-HA or control PSMC6-HA expressing vectors. Although variation was seen across the cell lines, downregulation of IRF4, MYC, CDK6 and upregulation of Igλ, BIP and *PBXIP1* were exclusively detected in FAM46C overexpressing cells (Figure 4C). BIP was upregulated after *FAM46C* introduction, but downstream proteins that mediated ER stress-induced apoptosis, such as CHOP/GADD153, was not elevated in FAM46C overexpressing cells. Finally, we found that two non-responsive cell lines, FR4 and JJN3, have no significant *IRF4* or *MYC* downregulation after exogenous *FAM46C* introduction (Figure 4D and 4E).

FAM46C mutation confers a survival or growth advantage to MM cells

Next, we investigated the functional effect of seven different *FAM46C* mutants previously published in MM patients and HMCLs(1, 7), including five missense, one nonsense and one frame shift mutations (Figure 5A). We also included a construct (#8) carrying a 14 amino acid in-frame deletion (residues 172 to 186), a region previously described as mutational hot spot(1). Lentiviruses expressing wild type and mutant constructs were prepared and used to infect MM1.S cells. FAM46C WT expression induced a 93% cell viability reduction at day 12 after infection (Figure 5B). Seven of eight FAM46C mutants showed less cytotoxicity than FAM46C WT. Accordingly, immunoblotting assay indicated that FAM46C WT induced the highest levels of IRF4 and MYC downregulation (Figure 5C). PolyPhen-2(30) mutational predictions correlated with viability assays (Figure 5D). Interestingly, mutation #4 (p.S115F) was predicted as a benign mutation and as predicted, demonstrated marked toxicity similar to that of WT FAM46C. To address the possibility that unnaturally high levels of virus induced FAM46C was responsible we also demonstrated that when exogenous wild type and mutant FAM46C were expressed at levels in OCIMY5 (which harbors a mono-allelic deletion of FAM46C) equivalent to the endogenous levels in XG1 (no deletion or mutation), only wild type FAM46C induced cell viability reduction (supplementary figure 2).

FAM46C deletion confers growth and survival advantages to MM cells

We next employed CRISPR-Cas9 to delete endogenous *FAM46C* in HMCLs. Seven gRNAs with the highest specificity were selected to target different regions of *FAM46C* (Figure 6A) and were lentivirally transduced into OCIMY5 cells. We sequenced *FAM46C* at day 4 and 14 after lentiviral infection and confirmed that all seven gRNAs targeted the endogenous *FAM46C* at the designed positions, producing indel mutations in an increasing percentage of infected cells from day 4 to day 14 (supplementary figure 3). Decreased FAM46C endogenous expression was detected in all gRNA lentivirus infected cells (supplementary figure 4). At five months after infection, no endogenous FAM46C was detected in four gRNAs-transduced cells (Figure 6B). Those cells (GFP positive) demonstrated a growth advantage when were admixed with parental, non-GFP, OCIMY5 cells (Figure 6C). We also isolated single clones that lack detectable FAM46C protein expression from five gRNAs infected pools (supplementary figure 5). These clones were isolated and grown over a period of two months. Twelve single surviving clones were tested by MTT assay and eight of them increased growth (ranging from 16%–49% increase in metabolic activity) compared with non-targeting control virus infected cells. We further studied drug response after *FAM46C*

knockout in two MM cell lines. As shown in figure 6D–E, depletion of FAM46C was shown to confer resistance to Dex (in both OCIMY5 and XG1) and Len (XG1 cells) treatment, but had no impact on bortezomib responsiveness. *FAM46C* CRISPR depletion induced activation of ERK and its downstream anti-apoptotic signaling, such as increasing BCL2 expression in XG1 and decreasing BIM expression in OCIMY5 (Figure 6F and supplementary figure 6). We also demonstrated that in XG1 and RPMI8226, that FAM46C depletion resulted in Ig light chain, BIP and MAGED1 downregulation (Figure 6G and supplementary figure 7). Gene expression analysis on two *FAM46C* depleted cell lines revealed 1005 altered transcripts (supplementary table 4). Significant alteration in signaling pathways affecting glucocorticoid and B cell receptor signaling, ATM signaling and protein ubiquitination pathways were present (supplementary table 5).

Discussion

FAM46C was recently identified as one of the most recurrently mutated genes in MM patients(3–7), however its function remains unknown. In the present study we confirmed that *FAM46C* is frequently mutated in HMCLs. Although FAM46C is predicted to localize in both, the cytoplasm and nucleus(11), we only detected protein in cytoplasmic extracts from four HMCLs, which is supportive of other recent reports, suggest that FAM46C function may be related to the regulation of mRNA stability in cytoplasm.

We further demonstrated that re-introduction of WT *FAM46C* in HMCLs carrying damaging *FAM46C* mutations induced substantial cytotoxicity. Conversely, the anti-myeloma activity induced by *FAM46C* overexpression is significantly reduced or abolished when a mutated *FAM46C* is employed. In our study, seven non-synonymous mutations (5 missense, 1 frame shift and 1 nonsense) previously identified in MM patients were cloned and introduced into MM cells. Six demonstrated impaired anti-myeloma activity compared with WT *FAM46C*, in accordance with a recent study, which suggested that the majority of *FAM46C* mutations found in MM patients are likely to affect FAM46 function domain (11). We demonstrated that endogenous *FAM46C* CRISPR-Cas9 knockout is not toxic but rather seems favorable for myeloma growth and confers resistance to dexamethasone and lenalidomide treatment. Together, these overexpression and deletion experiments indicate that mutation of *FAM46C* contribute to myeloma pathogenesis.

However, an analysis of MMRF coMMpass data, consistent with previously published data (6), did not detect a significant correlation of *FAM46C* expression or mutation with clinical overall survival (supplementary figure 8), although low FAM46C expression appears to associate with shorter response duration (supplementary figure 9). Thus while mutation confers MM survival it does not seem to impact outcomes after diagnosis.

Although the precise function of FAM46C is still unknown we have established some definitive areas for further investigation. For example, we demonstrated that *FAM46C* overexpression induced downregulation of several critical genes in MM survival, including *CEBPB, IRF4, and MYC*. The cell line FR4, which overexpresses *IRF4* as a consequence of an *IgH-IRF4* translocation, did not show viability reduction or IRF4/MYC downregulation after FAM46C overexpression. Moreover, OPM2 and LP1, which have high endogenous

IRF4 and CDK6 expression showed a delayed and less significant cytotoxicity after exogenous FAM46C introduction. In *FAM46C*-depleted MM cells, we found that expression of IRF4 and MYC were elevated or less responsive to dexamethasone or lenalidomide treatment compared with control. In addition, *FAM46C* knockout activated ERK signaling, an important pathway for myeloma cell proliferation and survival (31). Consistent with our work, a recent study demonstrated that expression of *FAM46C* was induced by treatment of hepatocellular carcinoma cells with an anti-tumor compound and expression of *FAM46C* was shown to associate with inhibition of ERK signaling(32).

Another interesting finding of this study was the upregulation of BIP, immunoglobulin light chain production and multiple genes involved in the UPR after FAM46C introduction, suggesting that *FAM46C* overexpression activates the ER stress pathway. FAM46C may regulate the UPR either directly through proteins associated with ER homeostasis or indirectly through upregulation of immunoglobulin production. Based on mRNA sequencing data, the inositol-requiring enzyme 1 (IRE-1) arm-mediated UPR is upregulated in *FAM46C* overexpressing cells, including upregulation of genes involving ER-associated protein degradation (such as *EDEM*), as well as genes that function in folding proteins such as protein disulfide isomerase (PDI)(33). However, not all downstream branches of the protein kinase RNA-like ER kinase (PERK) arm appear activated, e.g., ATF4 and CHOP/DDIT3, key molecules associated with ER stress-induced apoptosis, were not upregulated (34, 35). WT *FAM46C* induced the highest BIP and Ig upregulation when compared with most known clinical *FAM46C* mutants, which did not induce equivalent cytotoxicity or IRF4 and MYC downregulation as the wild type, further supporting that ER stress might be involved in initiating the FAM46C-mediated MM cytotoxicity.

Our study also supports that FAM46C is likely to physiologically involve in plasma cell Ig production and/or plasma cell differentiation. *FAM46C* overexpression induced lg light chain (λ in MM1.S, OPM2 and κ in KMS11) upregulation and secretion (LP1, supplementary figure 10), whereas FAM46C CRISPR-Cas9 induced Ig light chain downregulation. Indeed, *FAM46C* has been shown to be markedly upregulated during plasma cell differentiation(36). Interestingly, FAM46C overexpression induced downregulation of MYC, upregulation of Ig light chain and inhibition of certain branches of PERK are reminiscent of the final stages of plasma cell differentiation(37–39).

In summary, we demonstrated that *FAM46C* expression induces myeloma cytotoxicity and that *FAM46C* loss of function confers a growth and survival advantage to MM cells. These findings, together with sequencing data from MM patients, confirm that *FAM46C* mutation is engaged in myeloma pathogenesis or disease progression. We also demonstrated that FAM46C affects Ig production and genes regulating ER function suggesting a biological function related to plasma cell differentiation and ER homeostasis. Further studies are required on the identification of FAM46C binding partners and substrates, which will help us to fully understand FAM46C biological function and its pathological roles in MM development.

Supplementary Material

Refer to Web version on PubMed Central for supplementary material.

Acknowledgments

Financial support

This work was supported by the Mayo Clinic (A.K.S.), National Institutes of Health (A.K. Stewart, grant RO1CA183968-01A) and Spore Award (A.K. Stewart CA186781-02A1P4A).

We are grateful to Dr. Leif Bergsagel and Nizar J. Bahlis for insightful discussions and suggestions.

References

1. Boyd KD, Ross FM, Walker BA, Wardell CP, Tapper WJ, Chiecchio L, et al. Mapping of chromosome 1p deletions in myeloma identifies FAM46C at 1p12 and CDKN2C at 1p32.3 as being genes in regions associated with adverse survival. Clinical cancer research : an official journal of the American Association for Cancer Research. 2011; 17:7776–84. [PubMed: 21994415]
2. Walker BA, Leone PE, Chiecchio L, Dickens NJ, Jenner MW, Boyd KD, et al. A compendium of myeloma-associated chromosomal copy number abnormalities and their prognostic value. Blood. 2010; 116:e56–65. [PubMed: 20616218]
3. Chapman MA, Lawrence MS, Keats JJ, Cibulskis K, Sougnez C, Schinzel AC, et al. Initial genome sequencing and analysis of multiple myeloma. Nature. 2011; 471:467–72. [PubMed: 21430775]
4. Bolli N, Avet-Loiseau H, Wedge DC, Van Loo P, Alexandrov LB, Martincorena I, et al. Heterogeneity of genomic evolution and mutational profiles in multiple myeloma. Nature communications. 2014; 5:2997.
5. Lohr JG, Stojanov P, Carter SL, Cruz-Gordillo P, Lawrence MS, Auclair D, et al. Widespread genetic heterogeneity in multiple myeloma: implications for targeted therapy. Cancer cell. 2014; 25:91–101. [PubMed: 24434212]
6. Walker BA, Boyle EM, Wardell CP, Murison A, Begum DB, Dahir NM, et al. Mutational Spectrum, Copy Number Changes, and Outcome: Results of a Sequencing Study of Patients With Newly Diagnosed Myeloma. Journal of clinical oncology : official journal of the American Society of Clinical Oncology. 2015; 33:3911–20. [PubMed: 26282654]
7. Barbieri M, Manzoni M, Fabris S, Ciceri G, Todoerti K, Simeon V, et al. Compendium of FAM46C gene mutations in plasma cell dyscrasias. British journal of haematology. 2015
8. Kortum KM, Langer C, Monge J, Bruins L, Egan JB, Zhu YX, et al. Targeted sequencing using a 47 gene multiple myeloma mutation panel (M(3) P) in -17p high risk disease. British journal of haematology. 2015; 168:507–10. [PubMed: 25302557]
9. Kortum KM, Langer C, Monge J, Bruins L, Zhu YX, Shi CX, et al. Longitudinal analysis of 25 sequential sample-pairs using a custom multiple myeloma mutation sequencing panel (M(3)P). Annals of hematology. 2015; 94:1205–11. [PubMed: 25743686]
10. Kuchta K, Knizewski L, Wyrwicz LS, Rychlewski L, Ginalski K. Comprehensive classification of nucleotidyltransferase fold proteins: identification of novel families and their representatives in human. Nucleic acids research. 2009; 37:7701–14. [PubMed: 19833706]
11. Kuchta K, Muszewska A, Knizewski L, Steczkiewicz K, Wyrwicz LS, Pawlowski K, et al. FAM46 proteins are novel eukaryotic non-canonical poly(A) polymerases. Nucleic acids research. 2016; 44:3534–48. [PubMed: 27060136]
12. Schoggins JW, Wilson SJ, Panis M, Murphy MY, Jones CT, Bieniasz P, et al. A diverse range of gene products are effectors of the type I interferon antiviral response. Nature. 2011; 472:481–5. [PubMed: 21478870]
13. Ran FA, Hsu PD, Wright J, Agarwala V, Scott DA, Zhang F. Genome engineering using the CRISPR-Cas9 system. Nature protocols. 2013; 8:2281–308. [PubMed: 24157548]

14. Cong L, Ran FA, Cox D, Lin S, Barretto R, Habib N, et al. Multiplex genome engineering using CRISPR/Cas systems. Science. 2013; 339:819–23. [PubMed: 23287718]
15. Braggio E, Keats JJ, Leleu X, Van Wier S, Jimenez-Zepeda VH, Valdez R, et al. Identification of copy number abnormalities and inactivating mutations in two negative regulators of nuclear factor-kappaB signaling pathways in Waldenstrom's macroglobulinemia. Cancer research. 2009; 69:3579–88. [PubMed: 19351844]
16. Lipson D, Aumann Y, Ben-Dor A, Linial N, Yakhini Z. Efficient calculation of interval scores for DNA copy number data analysis. Journal of computational biology : a journal of computational molecular cell biology. 2006; 13:215–28. [PubMed: 16597236]
17. Kocher JP, Quest DJ, Duffy P, Meiners MA, Moore RM, Rider D, et al. The Biological Reference Repository (BioR): a rapid and flexible system for genomics annotation. Bioinformatics. 2014; 30:1920–2. [PubMed: 24618464]
18. Alcaide M, Tchigvintsev A, Martinez-Martinez M, Popovic A, Reva ON, Lafraya A, et al. Identification and characterization of carboxyl esterases of gill chamber-associated microbiota in the deep-sea shrimp Rimicaris exoculata by using functional metagenomics. Applied and environmental microbiology. 2015; 81:2125–36. [PubMed: 25595762]
19. Robinson JT, Thorvaldsdottir H, Winckler W, Guttman M, Lander ES, Getz G, et al. Integrative genomics viewer. Nature biotechnology. 2011; 29:24–6.
20. Kalari KR, Nair AA, Bhavsar JD, O'Brien DR, Davila JI, Bockol MA, et al. MAP-RSeq: Mayo Analysis Pipeline for RNA sequencing. BMC bioinformatics. 2014; 15:224. [PubMed: 24972667]
21. Trapnell C, Pachter L, Salzberg SL. TopHat: discovering splice junctions with RNA-Seq. Bioinformatics. 2009; 25:1105–11. [PubMed: 19289445]
22. Wang L, Wang S, Li W. RSeQC: quality control of RNA-seq experiments. Bioinformatics. 2012; 28:2184–5. [PubMed: 22743226]
23. Liao Y, Smyth GK, Shi W. featureCounts: an efficient general purpose program for assigning sequence reads to genomic features. Bioinformatics. 2014; 30:923–30. [PubMed: 24227677]
24. Livak KJ, Schmittgen TD. Analysis of relative gene expression data using real-time quantitative PCR and the 2(−Delta Delta C(T)) Method. Methods. 2001; 25:402–8. [PubMed: 11846609]
25. Shaffer AL, Emre NC, Lamy L, Ngo VN, Wright G, Xiao W, et al. IRF4 addiction in multiple myeloma. Nature. 2008; 454:226–31. [PubMed: 18568025]
26. Pal R, Janz M, Galson DL, Gries M, Li S, Johrens K, et al. C/EBPbeta regulates transcription factors critical for proliferation and survival of multiple myeloma cells. Blood. 2009; 114:3890–8. [PubMed: 19717648]
27. Dutta-Simmons J, Zhang Y, Gorgun G, Gatt M, Mani M, Hideshima T, et al. Aurora kinase A is a target of Wnt/beta-catenin involved in multiple myeloma disease progression. Blood. 2009; 114:2699–708. [PubMed: 19652203]
28. Tiedemann RE, Zhu YX, Schmidt J, Yin H, Shi CX, Que Q, et al. Kinome-wide RNAi studies in human multiple myeloma identify vulnerable kinase targets, including a lymphoid-restricted kinase, GRK6. Blood. 2010; 115:1594–604. [PubMed: 19996089]
29. Santo L, Hideshima T, Cirstea D, Bandi M, Nelson EA, Gorgun G, et al. Antimyeloma activity of a multitargeted kinase inhibitor, AT9283, via potent Aurora kinase and STAT3 inhibition either alone or in combination with lenalidomide. Clinical cancer research : an official journal of the American Association for Cancer Research. 2011; 17:3259–71. [PubMed: 21430070]
30. Adzhubei I, Jordan DM, Sunyaev SR. Predicting functional effect of human missense mutations using PolyPhen-2. Current protocols in human genetics / editorial board, Jonathan L Haines [et al]. 2013; Chapter 7(Unit7 20)
31. Chang-Yew Leow C, Gerondakis S, Spencer A. MEK inhibitors as a chemotherapeutic intervention in multiple myeloma. Blood cancer journal. 2013; 3:e105. [PubMed: 23524590]
32. Zhang QY, Yue XQ, Jiang YP, Han T, Xin HL. FAM46C is critical for the anti-proliferation and pro-apoptotic effects of norcantharidin in hepatocellular carcinoma cells. Scientific reports. 2017; 7:396. [PubMed: 28341836]
33. Oslowski CM, Urano F. Measuring ER stress and the unfolded protein response using mammalian tissue culture system. Methods in enzymology. 2011; 490:71–92. [PubMed: 21266244]

34. Harding HP, Zhang Y, Bertolotti A, Zeng H, Ron D. Perk is essential for translational regulation and cell survival during the unfolded protein response. Molecular cell. 2000; 5:897–904. [PubMed: 10882126]

35. Zinszner H, Kuroda M, Wang X, Batchvarova N, Lightfoot RT, Remotti H, et al. CHOP is implicated in programmed cell death in response to impaired function of the endoplasmic reticulum. Genes & development. 1998; 12:982–95. [PubMed: 9531536]

36. Affer M, Chesi M, Chen WD, Keats JJ, Demchenko YN, Tamizhmani K, et al. Promiscuous MYC locus rearrangements hijack enhancers but mostly super-enhancers to dysregulate MYC expression in multiple myeloma. Leukemia. 2014; 28:1725–35. [PubMed: 24518206]

37. Ma Y, Shimizu Y, Mann MJ, Jin Y, Hendershot LM. Plasma cell differentiation initiates a limited ER stress response by specifically suppressing the PERK-dependent branch of the unfolded protein response. Cell stress & chaperones. 2010; 15:281–93. [PubMed: 19898960]

38. Gass JN, Jiang HY, Wek RC, Brewer JW. The unfolded protein response of B-lymphocytes: PERK-independent development of antibody-secreting cells. Molecular immunology. 2008; 45:1035–43. [PubMed: 17822768]

39. Lin KI, Lin Y, Calame K. Repression of c-myc is necessary but not sufficient for terminal differentiation of B lymphocytes in vitro. Molecular and cellular biology. 2000; 20:8684–95. [PubMed: 11073970]

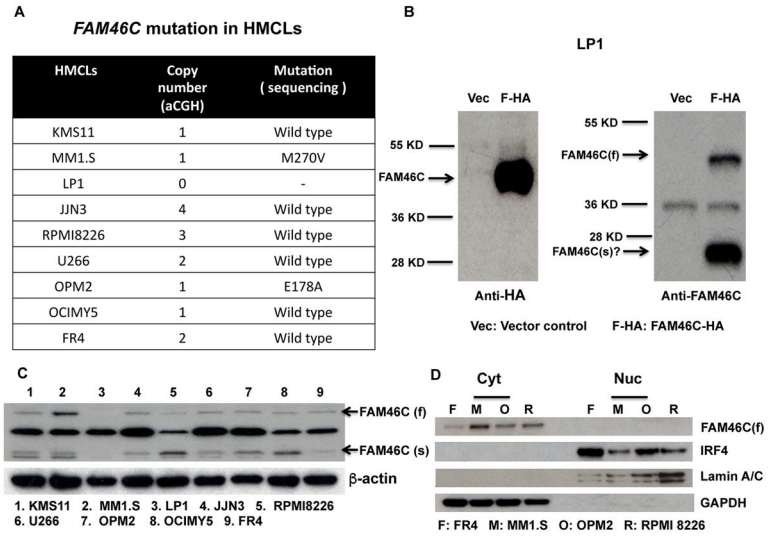

Figure 1. *FAM46C* is frequently mutated in HMCLs and endogenous FAM46C is located in cytoplasmic fraction

(**A**) The copy-number and mutation status of *FAM46C* in nine HMCLs were analyzed by aCGH and DNA sequencing. (**B**) The expression of *FAM46C* was analyzed in LP1 cells by immunoblotting. No endogenous FAM46C was detected in LP1 cells infected with control virus by anti-FAM46C. Both anti-HA and anti-FAM46C detected exogenous FAM46-HA in LP1 cells infected with lentivirus expressing FAM46C-HA. Anti-FAM46C also detected small band in addition to full-length (f) of FAM46C, it may represent short form (s) of FAM46C. (**C**) Endogenous FAM46C expression in those HMCLs was measured by immunoblotting assay with anti-FAM46C antibody. (**D**) The subcellular location of FAM46C in four HMCLs was analyzed by immunoblotting cytoplasmic and nuclear proteins with anti-FAM46C. Biochemical fractionation was performed as described in materials and methods, and analyzed by western blotting using the indicated antibodies. IRF4 and Lamin A/C were detected as nuclear protein markers and GAPDH was detected as cytoplasmic protein markers. Only full length of FAM46C was shown.

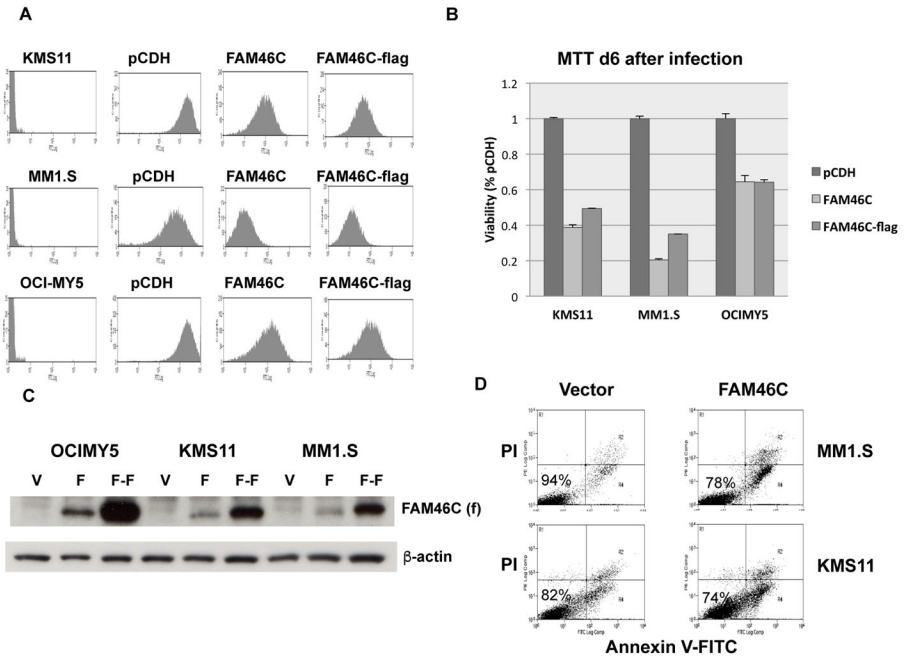

Figure 2. Overexpression of wild type *FAM46C* in MM cells induced cytotoxicity

Three HMCLs were infected with control (pCDH or vector) or FAM46C (F) expressing virus as described in methods. (**A**) Infection efficiency was measured at day 3 by FACS analysis of GFP expression, more than 80% cells were infected. (**B**) Cell viability was measured at day 6 after infection by MTT assay, it showed overexpression of both untagged (F) and Flag-tagged FAM46C (F-F) induced MM cytotoxicity. (**C**) FAM46C expression was measured by immunoblotting at day 3 after infection (with anti-FAM46C from Abcam). (**D**) Apoptosis assay was performed at day 3 after infection with control (vector) or FAM46C expressing virus using flow cytometry analysis, indicating that overexpression of FAM46C induced myeloma cytotoxicity.

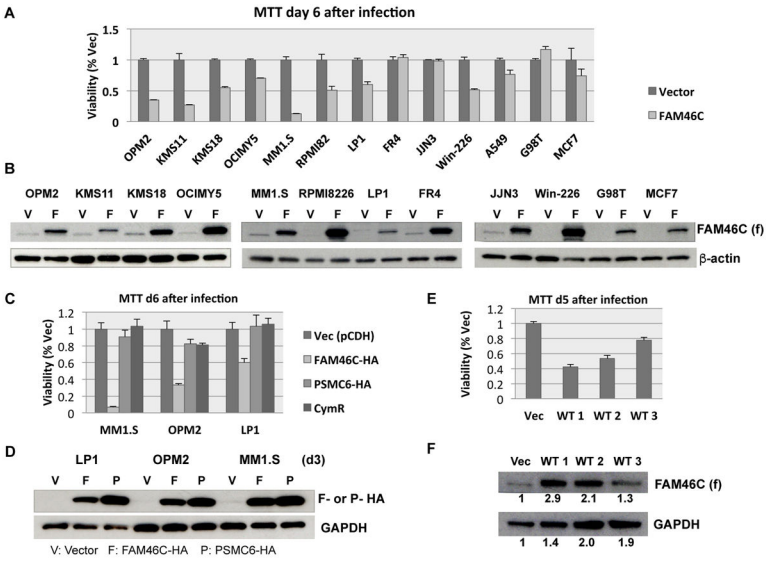

Figure 3. FAM46C-induced cytotoxicity was detected in the majority of myeloma cell lines tested, was dose dependent and specifically associated with *FAM46C* overexpression

(**A**) Nine myeloma and four non-myeloma cell lines were infected with control virus (pCDH or V) and FAM46C expressing virus (F) and cell viability was measured at day 6 after infection by MTT assay. A representative result was shown (the data was normalized to control for each cell line). (**B**) The expression of exogenous FAM46C was confirmed by immunoblotting assay. (**C**) Three HMCLs were infected with control virus or virus expressing FAM46C-HA, PSMC6-HA or CmyR repressor. The expression of HA-tagged FAM46C (F) and PSMC6 (P) was measured with anti-HA antibody at day 3 after infection. Cell viability was measured by MTT assay at day 6 after infection (**D**) and a substantial reduction of cell viability was only detected in FAM46C overexpressing cells. (**E**–**F**) FAM46C-induced cytotoxicity is dose dependent. MM1.S were infected with serially diluted virus expressing Flag-tagged FAM46C (from high WT1 to low WT 3) and compared with cells infected with vector virus (with high titer of virus) by MTT assay at day 5 and immunobloting assay with anti-FAM46C at day 3. Expression of FAM46C was normalized by the loading control (GAPDH) and quantified (number under images) by densitometry with Image J software (http://rsb.info.nih.gov/ij).

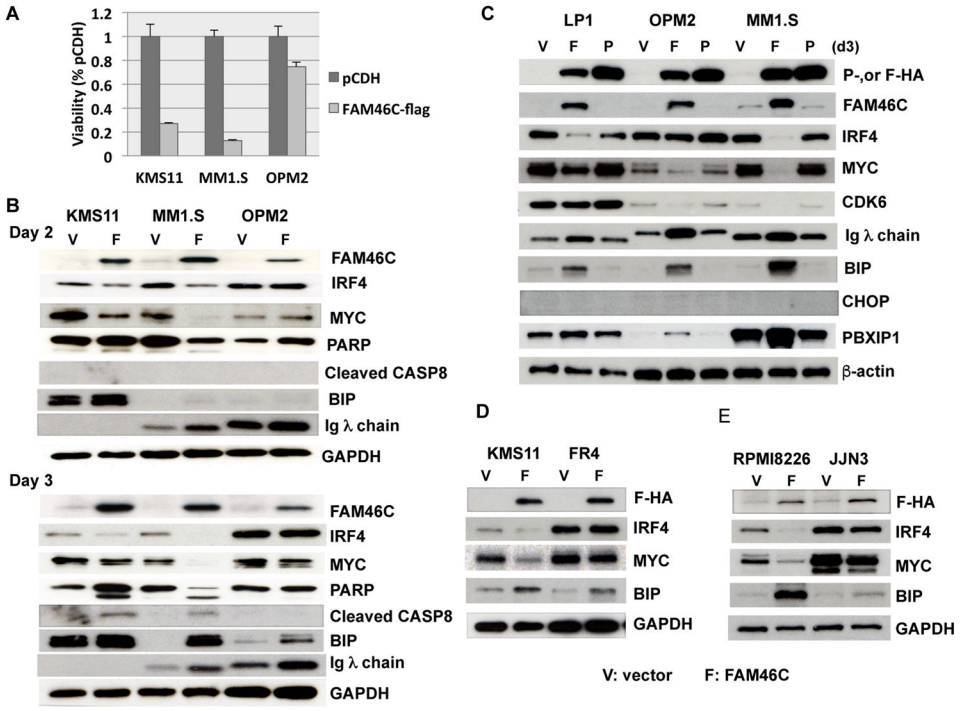

Figure 4. *FAM46C* overexpression induced IRF4 downregulation, lg light chain up-regulation and activation of UPR

(**A**) Three HMCLs were infected with the control virus (pCDH or V) or FAM46C (F) expressing virus. The cell viability was measured at day 6 after infection. (**B**) IRF-4, MYC, Caspase 8, PARP, Ig λ and BIP protein expression was measured at day 2 and day 3 after infection. (**C**) The protein changes were also measured in three cell lines at day 3 after infection of control virus (V) or virus expressing FAM46C-HA (F) or pSMC6-HA (P) by immunoblotting. (D–E) Two cell lines (FR4 and JJN3) that showed no cytotoxicity after *FAM46C* overexpression were analyzed by immunoblotting to compare with other cell lines.

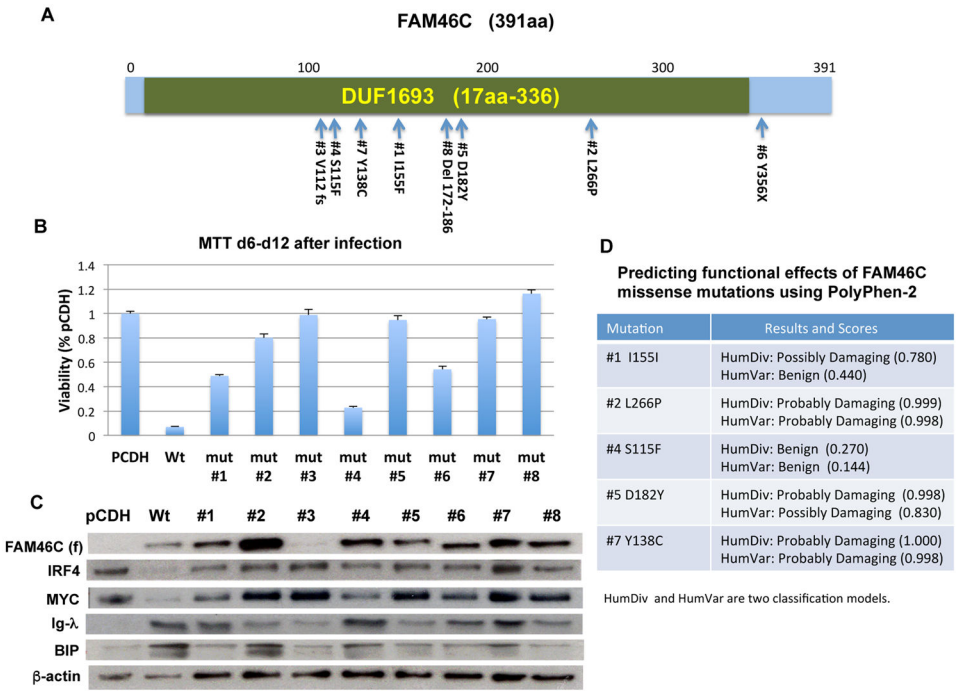

Figure 5. ***FAM46C*** **mutants previously identified in MM cells have no or reduced anti-myeloma activity**

(**A**) The schematic diagram of FAM46C protein and eight FAM46C mutants generated in this study. (**B**) MM1.S cells were infected with control virus (pCDH) and virus expressing wild type (Wt) or mutated FAM46C. At day 12 after infection, the viability of each infected cells was measured by MTT assay. (**C**) The expression of exogenous FAM46C and other proteins at day 3 after infection was analyzed by immunoblotting assay. (**D**) Five missense mutations tested above were analyzed using PolyPhen-2 software and the prediction results from two classification models are shown.

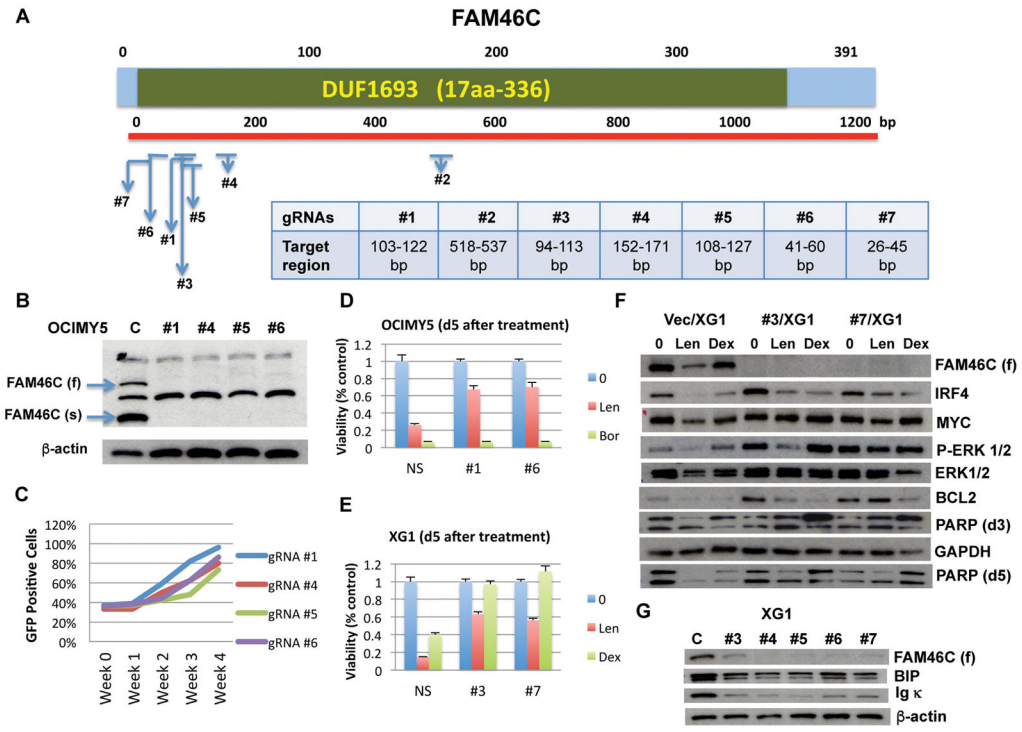

Figure 6. Knockout of FAM46C favors myeloma growth, survival and induces downregulation of Ig light chain and BIP

(**A**) The schematic diagram of FAM46C protein, cDNA and FAM46C gRNAs generated in this study. CRISPR-cas9 technology was used to knockout endogenous *FAM46C* in MM cells. (**B**) The expression of *FAM46C* in #1, #4, #5 and #6 gRNA transduced OCIMY5 cells were examined at five months after infection by immunoblotting. No FAM46C protein (both full length and short form) was detected in those cells. (**C**) The FAM46C deficient cells (GFP^+) were admixed 30:70 with parental OCIMY5 (GFP^-), followed by flow cytometry analysis of the percent of surviving GFP^+ population weekly. *FAM46C* deleted cells have growth advantage compared with parental cells. (**D–E**) OCIMY5 and XG1 cells harboring control virus (NS) or two FAM46C gRNAs were treated without or with dexamethasone (5μM for XG1 and 10 μM for OCIMY5), Lenalidomide (5 μM, XG1) and Bortezomib (3.5nM, OCIMY5), and then cell viability was measured by MTT assay at day 5. The cells treated at the same condition were also harvested at day 3 for Immunoblotting assay (**F). (G)** XG1 cells were infected with control virus and lentivirus expressing indicated FAM46C CRISPRs. The protein lysate prepared from those infected cells at one and two months after infection was analyzed by immunoblotting. The expression of Ig light chain and BIP was decreased in FAM46C CRISPRs transduced cells.

Table 1

Pathway analysis of the genes whose expression was significantly altered after introduction of FAM46C in MM cells

Ingenuity Canonical Pathways	p-value
Mitochondrial Dysfunction	1.41E-07
Unfolded protein response	6.76E-06
Antigen Presentation Pathway	5.75E-05
Lipid Antigen Presentation by CD1	1.05E-04
NRF2-mediated Oxidative Stress Response	1.51E-04
phagosome maturation	4.27E-04
Dolichyl-diphosphooligosaccharide Biosynthesis	7.08E-04
tRNA Charging	7.59E-04
Oxidative Phosphorylation	1.00E-03
Aryl Hydrocarbon Receptor Signaling	1.29E-03
Glutathione Redox Reactions II	2.04E-03
Aldosterone Signaling in Epithelial Cells	2.24E-03
Tetrahydrofolate Salvage from 5,10-methenyltetrahydrofolate	3.31E-03
Prostate Cancer Signaling	4.37E-03
Chondroitin and Dermatan Biosynthesis	5.01E-03

MM1.S and KMS11 cells were harvested at day 3 after infection with lentivirus harboring either control vector or wild-type FAM46C-expressing cassette and analyzed by mRNA-seq assay. Differential analysis was then performed by Student's t-test for two comparisons (MM1.S FAM46C vs. control, KMS11 FAM46C vs. control). Genes determined as differentially expressed were submitted to Ingenuity Pathway Analysis (IPA,http://www.ingenuity.com/) for pathway enrichment analysis. The top canonical pathways significantly affected by FAM46C overexpression were identified and listed.